

Regular Article

Performance Experiments of the Humidity Control System in the ^{220}Rn Chamber

Atsuyuki Sorimachi^{1,3*}, Tetsuo Ishikawa^{2,3} and Shinji Tokonami¹

¹*Department of Radiation Physics, Institute of Radiation Emergency Medicine, Hirosaki University,
66-1 Hon-cho, Hirosaki 036-8564, Japan*

²*National Institute of Radiological Sciences, 4-9-1 Anagawa, Inage-ku, Chiba 263-8555, Japan*

³*Fukushima Medical University, 1 Hikarigaoka, Fukushima 960-1295, Japan*

Received 19 December 2013; revised 13 February 2014; accepted 19 March 2014

This paper describes performance experiments of a humidity control system in a thoron ^{220}Rn chamber which adjusts and controls the humidity inside the chamber. The easily constructed and used humidity control system has a perfluorosulfonic membrane (commercially known as Nafion[®]) tube as the air humidity conditioner. The tube includes tube moisture exchangers that allow the transfer of water vapor between a flowing sample gas stream and a flowing purge gas stream over the exterior surface of the tube. Thus the tube has an advantage of being able to adjust the sample air flow to the desired humidity conditions. We investigated the optimal operation of the air humidity conditioner, including such items as response time to humidity, ability to control the humidity in the air and the losses of ^{220}Rn gas in passing through the air humidity conditioner. Our first experiment showed that the performance of the air humidity conditioner depended on the flow rate conditions of sample and purge air flows. Only small losses due to decay of ^{220}Rn and adsorption of ^{220}Rn gas onto the tube surfaces were also evident. In the second experiment with the ^{220}Rn chamber, we were able to adjust and control the humidity in the chamber using the humidity control system with the air humidity conditioner.

Key words: humidity, Nafion[®]; sulfonic acid, thoron, time constant

1. Introduction

Thoron (^{220}Rn) is a natural radon (^{222}Rn) isotope with a relatively short half-life (55.6 s), comparing with ^{222}Rn (3.82 days). Although United Nations Scientific Committee on the Effects of Atomic Radiation (UNSCEAR) reports estimated that the contribution of ^{220}Rn and its progeny to the total annual effective dose from ^{222}Rn was about 8%^(1, 2),

in some cases the dose contribution due to the inhalation of ^{220}Rn and its progeny could equal to or even exceeded that of ^{222}Rn and its progeny⁽³⁾. In order to determine the radiation hazard from ^{220}Rn and its progeny, it is necessary to make accurate measurements in indoor surveys using proper detectors. Determining the radiation hazard from ^{220}Rn and its progeny has become imperative from the viewpoint of radiation protection. Additionally, developing an accurate measurement procedure for ^{220}Rn and its progeny would be beneficial, because such measurements are overestimated due to interference from ^{220}Rn and its progeny⁽⁴⁾.

Passive time-integrating ^{222}Rn - ^{220}Rn discriminative

*Atsuyuki Sorimachi: Fukushima Medical University
1 Hikarigaoka, Fukushima 960-1295, Japan
E-mail: sorimac@fmu.ac.jp

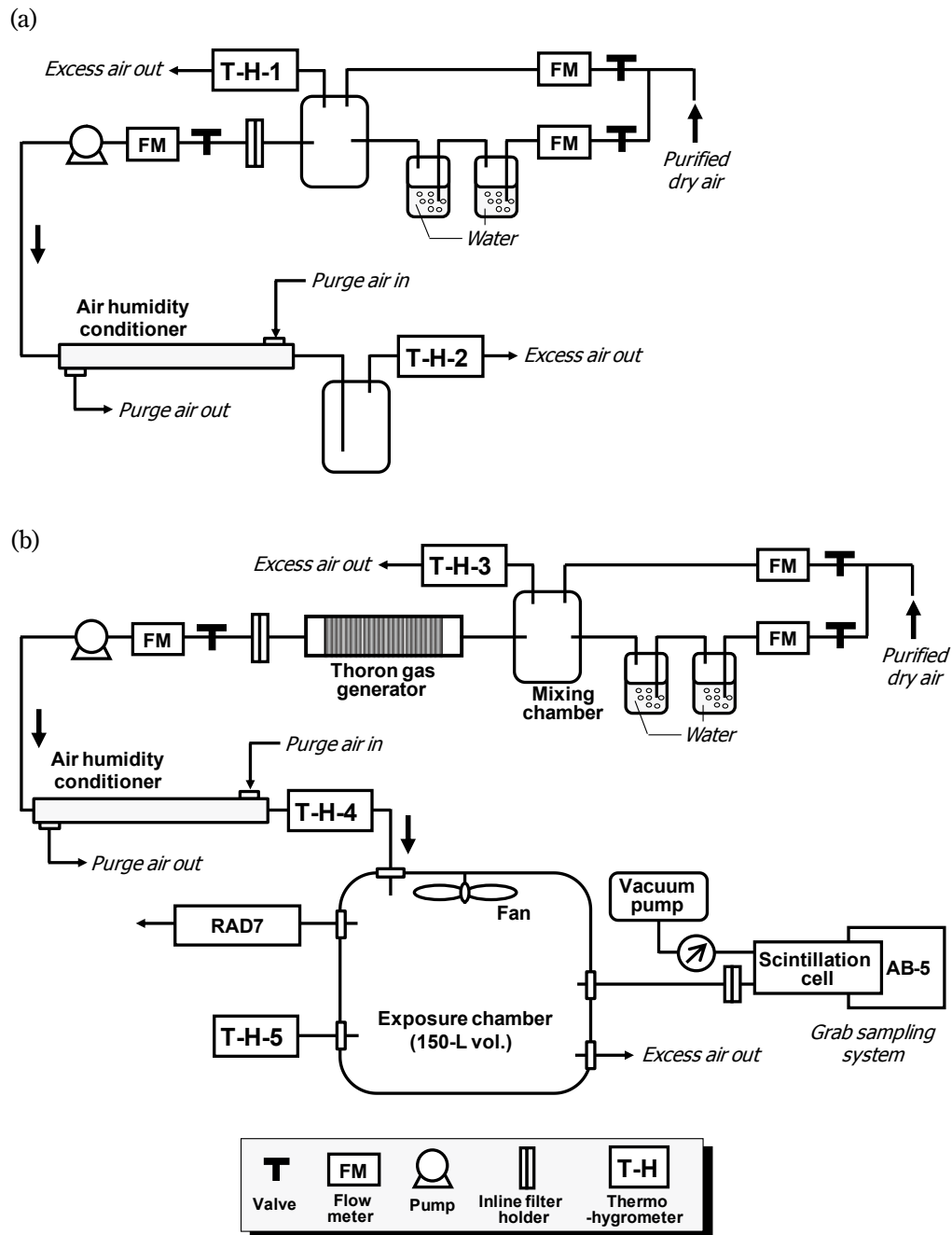


Fig. 3. Schematic diagrams of the experimental setup in (a) the performance experiments for the humidity control system and (b) ^{220}Rn gas generation with the humidity control system.

The chamber air temperature and relative humidity (RH) were monitored at 1-min intervals using a hygrometer Model TR-73U (T & D Corporation, Japan).

In order to evaluate the characteristics of humidity in the air in the ^{220}Rn chamber using the air humidity conditioner, the ^{220}Rn chamber system of National Institute of Radiological Sciences (NIRS)^{21, 22)} was used (Fig. 3b). The ^{220}Rn concentrations were measured once every hour using an electrostatic collection (EC) monitor,

the RAD7 (DurrIDGE Co. Inc., U.S.A.). In addition to this continuous measurement, intermittent measurements by grab sampling were also made during the experiment using a ZnS scintillation cell (SC) Model 300A (inner volume: 270 mL) with a portable radiation monitor Model AB-5 (Pylon Electronics Inc., Canada) so as to obtain the quality assurances of the measured ^{220}Rn concentration¹⁹⁾. The chamber air temperature and RH were monitored at 1-h intervals using a hygrometer Model HygroPalm-2

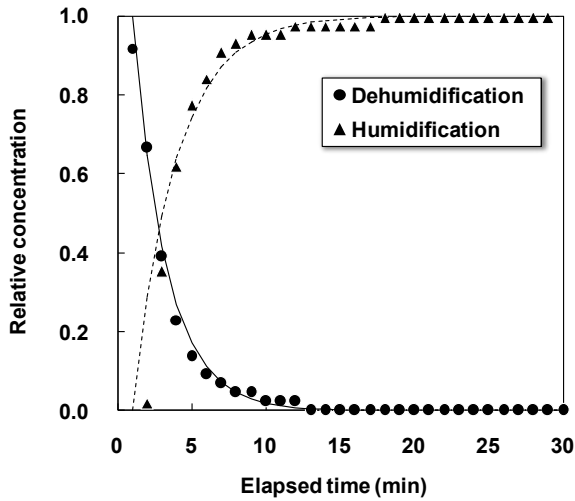


Fig. 4. Responses of the air humidity conditioner to humidity step changes at dehumidification and humidification experiments. The solid and dashed lines are fits of Eqs. 1 and 2 to measurements, respectively.

(ROTRONIC AG, Switzerland) for the ^{220}Rn chamber.

3. Results and discussion

3.1. Performance experiments of air humidity conditioner

In the ^{220}Rn chamber the flow rate through the ^{220}Rn source was set to about 2 L min^{-1} during generation of ^{220}Rn gas to take into account configuration of the ^{220}Rn chamber²¹). Accordingly, in this study performance experiments of the air humidity conditioner were carried out at the flow rate from 0.5 to 2 L min^{-1} .

In order to derive the response time of the air humidity conditioner, humidified and dried air flows were introduced to the air humidity conditioner for the sample and purge air flows (dehumidification experiments), respectively, and vice versa (humidification experiments).

For the first-order response the formulas for the dehumidification and humidification experiments are Eqs. 1 and 2, respectively,

$$f(t) = \frac{C_{\text{Outlet}}}{C_{\text{Inlet}}} = \exp\left(-\frac{t-t_0}{\tau}\right) \quad (1)$$

$$f(t) = \frac{C_{\text{Outlet}}}{C_{\text{Inlet}}} = 1 - \exp\left(-\frac{t-t_0}{\tau}\right) \quad (2)$$

where C_{Inlet} and C_{Outlet} are the RHs at the inlet and outlet of the air humidity conditioner in %, respectively, t is time in min, t_0 is time of the humidity step in min and τ is system time constant in min. τ is fitted to dehumidification experiments at time, t_0 , and the analogue exponential growth model to humidification experiments at time, t_0 , in order to determine τ of the system. With the applied

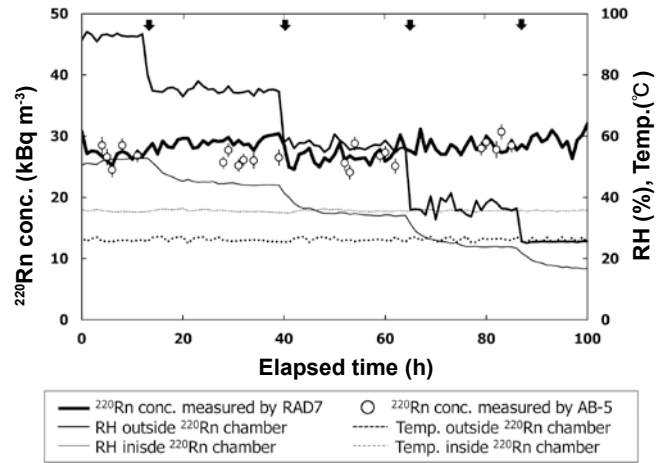


Fig. 5. Time variation of ^{220}Rn concentrations, temperature and relative humidity using the air humidity conditioner. Two sets of air humidity conditioners were used. The flow rates of sample and purge air flows of the air humidity conditioner were set to 1 and 2 L min^{-1} , respectively. The arrows show the time when the humidity in the purge air flow was changed.

exponential mode, a 95% signal response is achieved after 3τ .

Figure 4 exemplifies the response of the air humidity conditioner to the humidity step change at dehumidification and humidification experiments. The mean (\pm standard deviation) temperature was $25.4 \pm 0.5 \text{ }^\circ\text{C}$ within 2% relative standard deviation (RSD) for all experiments. As shown in the graph, the measured points at both dehumidification and humidification experiments were fitted to the Eqs. 1 and 2, respectively, in order to determine τ of the air humidity conditioner.

For the flow rate of sample air flow at a constant flow rate of purge air flow (runs 1 and 4, 3 and 5), the equilibrium RH and τ at dehumidification experiments became higher with increasing the flow rate of sample air flow. The inverse tendency at humidification experiments was observed for the equilibrium RH. This indicates that the higher flow rate ratio of purge to sample air flows exchanged more water vapor over the exterior surface of the tube, and consequently, lower (higher) equilibrium RH at dehumidification (humidification) experiments was achieved and faster response was found.

The variability in equilibrium RH and τ associated with the flow rate ratio of purge to sample air flows was examined. By increasing the flow rate of purge air flow at a constant sample flow rate of 1 L min^{-1} (runs 1, 2 and 3), which means the flow rate ratio of purge to sample air flows, a decrease in equilibrium RH at dehumidification experiments and the increase at humidification experiments was observed, while the corresponding τ values seemed to become short at both experiments. Thus equilibrium RH and τ of the sample air flow depended on the flow rate ratio of purge to sample air

Table 1. Equilibrium relative humidity (RH) and time constant (τ) at given flow rates of sample and purge air flows of the air humidity conditioner ($F_{\text{Sam.}}$ and $F_{\text{Pur.}}$) at dehumidification and humidification experiments^a

Run	$F_{\text{Sam.}}$ (L min ⁻¹)	$F_{\text{Pur.}}$ (L min ⁻¹)	N ^b	Dehumidification experiment			Humidification experiment		
				$C_{\text{inlet}}^{\text{c, d}}$ (%)	$C_{\text{Eq.}}^{\text{c}}$ (%)	τ (min)	$C_{\text{inlet}}^{\text{c, d}}$ (%)	$C_{\text{Eq.}}^{\text{c}}$ (%)	τ (min)
1	1	0.5	1	95	61 (1)	5.4 (0.0)	10	26 (1)	7.1 (2.7)
2	1	1	1	95	55 (2)	2.8 (0.4)	10	40 (2)	3.3 (0.3)
3	1	2	1	95	54 (2)	3.1 (1.1)	10	52 (1)	3.0 (0.1)
4	0.5	0.5	1	95	43 (1)	4.1 (0.7)	10	53 (1)	3.5 (0.2)
5	2	2	1	95	65 (4)	3.6 (0.6)	10	34 (0)	2.1 (0.2)
6	1	2	2 ^e	95	36 (1)	2.6 (0.2)	10	76 (3)	2.7 (0.0)

^a Values in parentheses are standard deviations ($n = 2$ except run 2 ($n = 4$)).

^b Number of air humidity conditioners.

^c C_{inlet} and $C_{\text{Eq.}}$ represent the RH at the inlet of the air humidity conditioner and the equilibrium RH measured at the outlet of the air humidity conditioner, respectively. The RHs at the inlet and outlet of the air humidity conditioner were measured using the hygrometers "T-H-1" and "T-H-2" shown in Fig. 3a, respectively.

^d Detectable range of the Model TR-73U hygrometer ranged from 10 to 95% RH. When the readings from the hygrometers were out of the detectable range, the values of C_{inlet} were represented as upper and lower detection limits.

^e Two sets of air humidity conditioners were connected in series.

Table 2. Mean (standard deviation) ²²⁰Rn concentration and relative humidity (RH) in the ²²⁰Rn chamber using two sets of air humidity conditioners^a

RH ^b (%)	²²⁰ Rn concentration ^c			²²⁰ Rn ratio of EC to Cal. (-)
	EC	SC (kBq m ⁻³)	Cal.	
52.5 (0.2)	27.2 (1.3)	25.8 (0.5)	25.8 (0.5)	1.05 (0.05)
44.7 (0.7)	29.0 (0.8)	26.2 (0.9)	26.5 (0.9)	1.09 (0.05)
34.6 (0.7)	26.8 (1.3)	26.5 (0.8)	26.5 (0.8)	1.01 (0.06)
24.3 (0.8)	28.2 (1.1)	27.0 (1.0)	27.0 (1.0)	1.04 (0.06)
17.2 (0.4)	29.4 (1.4)	NM ^d	26.0 (0.9)	1.13 (0.07)
RSD (%) ^e	4.0	1.9	1.8	

^a All data are derived from Fig. 5.

^b The values were the equilibrium RH after changing RH outside the chamber. The RH in the ²²⁰Rn chamber was measured using the hygrometer "T-H-5" shown in Fig. 3b.

^c "EC", "SC" and "Cal." respectively represent the ²²⁰Rn concentrations measured by the RAD7 electrostatic collection monitor, the 300A scintillation cell with the AB-5 portable radiation monitor, and calculated from the equation reported by Sorimachi et al.²¹⁾ [$C_{\text{Tn}} = 0.592\exp(0.234\text{AH})$], where C_{Tn} and AH are the ²²⁰Rn concentration and absolute humidity in the chamber, respectively].

^d Not measured.

^e Relative standard deviation.

flows of the air humidity conditioner.

The effect of the number of air humidity conditioner on the variability in equilibrium RH and τ was investigated (runs 3 and 6). From Table 1, the efficiency of both dehumidification and humidification experiments by the air humidity conditioner increased by approximately 30% with an increase of the number of air humidity conditioners.

3.2. Time variation of ²²⁰Rn and RH in the ²²⁰Rn chamber using the air humidity conditioner

The variations of the temperature and RH are plotted as a function of time in Figure 5. Using Figure 3b, we graduated the RH outside the chamber from 93% to 26% by passing through two sets of air humidity conditioners in series at sample and purge flow rates of 1 and 2 L min⁻¹, respectively. As a result, a systematic temporal

pattern was observed that the RH inside the chamber decreased with time until achieving equilibrium within the first 6 h after changing the humidity outside the chamber. Using Eq. 1, we estimated τ for the chamber to be approximately 4 h. These may correspond to the residence time in the ²²⁰Rn chamber (2.5 h) and the time to reach equilibrium of adsorption and desorption of water vapor on the chamber surfaces. Accordingly, the air humidity conditioner was able to make adjustments from 17 to 53% RH inside the ²²⁰Rn chamber by changing outside RH from 26 to 93%.

The variations of ²²⁰Rn concentrations are also plotted as a function of time in Figure 5. The ²²⁰Rn concentration remained nearly constant for about 100 h, with RSD of 4%. This stability of the ²²⁰Rn concentration was in agreement with results reported by Sorimachi *et al.*²¹⁾

The adsorption of ²²⁰Rn gas in the sample air on the

interior surfaces of the tube was evaluated. From Table 2, the ^{220}Rn concentration with the air humidity conditioner at each RH level was $28.1 (\pm 1.1) \text{ kBq m}^{-3}$, which was measured by the RAD7 monitor. On the other hand, the estimated ^{220}Rn concentration without the air humidity conditioner was $26.4 (\pm 0.5) \text{ kBq m}^{-3}$, which was calculated from the expression reported by Sorimachi *et al.*²¹ [$C_{\text{Tn}} = 0.592 \exp(0.234 \text{ AH})$, where C_{Tn} and AH were the ^{220}Rn concentration and absolute humidity in the chamber, respectively]. From Table 2, the ^{220}Rn concentration ratio of the measured value to the estimated value was constant with a value of approximately 1 at 17–53% RH. At a sample flow rate of 1 L min^{-1} with one air humidity conditioner, the losses of ^{220}Rn gas due to decay were less than 0.1%. Thus, the losses of ^{220}Rn gas can be ignored in passing the air through the air humidity conditioner.

4. Conclusions

We have established and performed the humidity control system using the Nafion[®] tube as the air humidity conditioner in the ^{220}Rn chamber. The conditioner has an advantage of being able to adjust the sample air flow to the desired humidity conditions. Consequently, there were only small losses due to decay of ^{220}Rn gas and adsorption of ^{220}Rn gas in the sample gas on the tube surfaces. The humidity control system was also able to adjust and control the humidity in the ^{220}Rn chamber. The feature of the ^{220}Rn chamber with the humidity control system satisfies the experimental conditions carried out in the calibration experiments²⁹, intercomparison experiments^{30, 31} and performance experiments of the passive radon and thoron detectors^{24–26} and then is available to similar experiments to them. Thus the technique established through the present study may be able to supply useful information about the generation technique of ^{220}Rn gas in the ^{220}Rn chamber for calibration and performance checks of passive time-integrating detectors.

Acknowledgments

This work was partly supported by a Grant-in-Aid for Young Scientists (Start-up) from Japan Society for the Promotion of Science (20810045) from the Ministry of Education, Culture, Sports, Science and Technology of Japan.

References

1. United Nations Scientific Committee on the Effects of Atomic Radiation (2000) Sources and effects of ionizing radiation. 2000 Report to the General Assembly. New York: United Nations.
2. United Nations Scientific Committee on the Effects of Atomic Radiation (2006) Effects of ionizing radiation. 2006 Report to the General Assembly. New York: United Nations.
3. Schery SD (1990) Thoron in the environment. *J Air Waste Manage Assoc* 40: 493–497.
4. Tokonami S (2010) Why is ^{220}Rn (thoron) measurement important? *Radiat Prot Dosimetry* 141: 335–339.
5. Zhuo W, et al. (2002) A simple passive monitor for integrating measurements of indoor thoron concentrations. *Rev Sci Instrum* 73: 2877–2881.
6. Tokonami S, et al. (2005) Up-to-date radon-thoron discriminative detector for a large scale survey. *Rev Sci Instrum* 76: 113505–1–113505–5.
7. Tokonami S, et al. (2004) Radon and thoron exposures for cave residents in Shanxi and Shaanxi provinces. *Radiat Res* 162: 390–396.
8. Tokonami S, et al. (2005) Natural radiation levels in Tamil Nadu and Kerala, India. *Radioact Environ* 7: 554–559.
9. Sugino M, et al. (2005) Radon and thoron concentrations in offices and dwellings of the Gunma prefecture, Japan. *J Radioanal Nucl Chem* 266: 205–209.
10. Kim C-K, et al. (2007) ^{220}Rn and its progeny in dwellings of Korea. *Radiat Meas* 42: 1409–1414.
11. Kávási N, et al. (2007) Radon and thoron parallel measurements in Hungary. *Radiat Prot Dosimetry* 123: 250–253.
12. Chen J, et al. (2008) Preliminary results of simultaneous radon and thoron tests in Ottawa. *Radiat Prot Dosimetry* 130: 253–256.
13. Chen J, et al. (2011) Characteristics of thoron and thoron progeny in Canadian homes. *Radiat Environ Biophys* 50: 85–89.
14. Chen J, et al. (2012) Determination of thoron equilibrium factor from simultaneous long-term thoron and its progeny measurements. *Radiat Prot Dosimetry* 149: 155–158.
15. Ramola RC, et al. (2010) Preliminary indoor thoron measurements in high radiation background area of southeastern coastal Orissa, India. *Radiat Prot Dosimetry* 141: 379–382.
16. Ramola RC, et al. (2012) Levels of thoron and progeny in high background radiation area of southeastern coast of Odisha, India. *Radiat Prot Dosimetry* 152: 62–65.
17. McLaughlin J, et al. (2011) Long-term measurements of thoron, its airborne progeny and radon in 205 dwellings in Ireland. *Radiat Prot Dosimetry* 145: 189–193.
18. Tokonami S, et al. (2001) Contribution from thoron on the response of passive radon detectors. *Health Phys* 80: 612–615.
19. Tokonami S, et al. (2002) Simple, discriminative measurement technique for radon and thoron concentrations with a single scintillation cell. *Rev Sci Instrum* 73: 69–72.
20. Sorimachi A, et al. (2008) Performance of NIRS thoron chamber system. *AIP Conf Proc* 1034: 206–209.
21. Sorimachi A, et al. (2009) Generation and control of thoron emanated from lantern mantles. *Rev Sci Instrum* 80: 015104–1–015104–4.
22. Sorimachi A, et al. (2010) Quality assurance and quality control for thoron measurement at NIRS. *Radiat Prot Dosim* 141: 367–370.
23. Sorimachi A, et al. (2012) Performance test of passive radon-thoron discriminative detectors on environmental parameters. *Radiat Meas* 47: 438–442.
24. Bochicchio F, et al. (2009) Sensitivity to thoron of an SSNTD-based passive radon measuring device: experimental evaluation and implications for radon concentration measurements and risk assessment. *Radiat Meas* 44: 1024–1027.
25. Sorimachi A, et al. (2009) Influence of the presence of humidity, ambient aerosols and thoron on the detection responses of electret

- radon monitors. *Radiat Meas* 44: 111–115.
26. Chen J, et al. (2010) An investigation on radon and thoron response of alpha-track detectors used in the Winnipeg case-control study. *Radiat Prot Dosim* 138: 83–86.
 27. Vargas A, Ortega X (2007) Influence of environmental changes on integrating radon detectors: results of an intercomparison exercise. *Radiat Prot Dosim* 123: 529–536.
 28. Perma Pure LLC. <http://www.permapure.com>. Accessed December 9, 2013.
 29. Tokonami S, et al. (2008) The Japanese radon and thoron reference chambers. *AIP Conf Proc* 1034: 202–205.
 30. Sorimachi A, et al. (2012) An intercomparison for NIRS and NYU passive thoron gas detectors at NYU. *Health Phys* 102: 419–424.
 31. Janik M, et al. (2010) International intercomparisons of integrating radon/thoron detectors with the NIRS radon/thoron chambers. *Radiat Prot Dosim* 141: 436–439.